GR-KLF15 pathway controls hepatic lipogenesis during fasting

Yoshinori Takeuchi[1,2,3], Yuki Murayama[1,2], Yuichi Aita[1,2], Zahra Mehrazad Saber[1,2], Samia Karkoutly[1,2], Duhan Tao[1,2], Kyoka Katabami[1,2], Chen Ye[1,2], Akito Shikama[1,2], Yukari Masuda[1], Yoshihiko Izumida[1], Takafumi Miyamoto[2], Takashi Matsuzaka[2], Yasushi Kawakami[2], Hitoshi Shimano[2] (iD) and Naoya Yahagi[1,2,3] (iD)

1 Nutrigenomics Research Group, Institute of Medicine, University of Tsukuba, Tsukuba, Japan
2 Department of Endocrinology and Metabolism, Institute of Medicine, University of Tsukuba, Tsukuba, Japan
3 Division of Endocrinology and Metabolism, Department of Internal Medicine, School of Medicine, Jichi Medical University, Shimotsuke, Japan

During periods of fasting, the body undergoes a metabolic shift from carbohydrate utilization to the use of fats and ketones as an energy source, as well as the inhibition of *de novo* lipogenesis and the initiation of gluconeogenesis in the liver. The transcription factor sterol regulatory element-binding protein-1 (SREBP-1), which plays a critical role in the regulation of lipogenesis, is suppressed during fasting, resulting in the suppression of hepatic lipogenesis. We previously demonstrated that the interaction of fasting-induced Kruppel-like factor 15 (KLF15) with liver X receptor serves as the essential mechanism for the nutritional regulation of SREBP-1 expression. However, the underlying mechanisms of KLF15 induction during fasting remain unclear. In this study, we show that the glucocorticoid receptor (GR) regulates the hepatic expression of KLF15 and, subsequently, lipogenesis through the KLF15-SREBP-1 pathway during fasting. KLF15 is necessary for the suppression of SREBP-1 by GR, as demonstrated through experiments using KLF15 knockout mice. Additionally, we show that GR is involved in the fasting response, with heightened binding to the KLF15 enhancer. It has been widely known that the hypothalamic–pituitary–adrenal (HPA) axis regulates the secretion of glucocorticoids and plays a significant role in the metabolic response to undernutrition. These findings demonstrate the importance of the HPA-axis-regulated GR-KLF15 pathway in the regulation of lipid metabolism in the liver during fasting.

Introduction

Maintaining life requires energy and the body derives its energy from the controlled combustion of three macronutrients, that is, carbohydrate, fat, and protein, and regulation of metabolic fuel selection plays a prominent role in the physiological adaptation to fasting. During fasting, fuel utilization shifts from carbohydrate to fat and ketone oxidation, which accompanies decreasing carbohydrate oxidation and switching to fat and protein metabolism to provide the metabolic fuels of the body [1]. These metabolic changes include the shutdown of *de novo* lipogenesis as well as the start-up of gluconeogenesis in the liver.

The *de novo* lipogenesis, the conversion of carbohydrate to fat, is mainly controlled by sterol regulatory

Abbreviations

ACTH, adrenocorticotropic hormone; ADX, adrenalectomy; ChIP, chromatin immunoprecipitation; Cort, corticosterone; Dex, dexamethasone; GR, glucocorticoid receptor; GRE, GR-binding element; HPA, hypothalamic–pituitary–adrenal; KLF15, Kruppel-like factor 15; LXR, liver X receptor; SREBP-1, sterol regulatory element-binding protein-1; TG, triglyceride.

element-binding protein-1 (SREBP-1) in the liver [2–6]. As a transcription factor, SREBP-1 targets various genes involved in the fatty acid synthesis pathway, such as *Fasn* (encoding fatty acid synthase: FAS) and *Acaca* (encoding acetyl-CoA carboxylase: ACC), and plays an important role in lipogenesis by controlling their gene expression. In particular, fasting remarkably reduces mRNA expression and thereby the amount of nuclear protein of SREBP-1 in the liver, which leads to the shutdown of hepatic lipogenesis during fasting [7].

Previously, we reported that the Kruppel-like factor 15 (KLF15) interaction with liver X receptor (LXR) serves as the essential mechanism for the nutritional regulation of sterol regulatory element-binding protein-1 (SREBP-1) expression during fasting [8]. Rapid induction of KLF15 during fasting contributes to the regulation of hepatic gluconeogenesis and amino acid catabolism [9–13] as well as lipogenesis [8]. In addition, we demonstrated that the forkhead box O-class (FoxO) subfamily of forkhead transcription factors, specifically FoxO1 and FoxO3a, has an impact on the fasting-induced upregulation of liver-specific KLF15 transcript, KLF15-1a [14,15].

As another important regulator of KLF15, glucocorticoid receptor (GR), a member of the nuclear receptor family, has been known to play a role in skeletal muscle [16,17], adipocytes [18], and brain [19]. The corticosteroids, cortisol in humans and corticosterone (Cort) in rodents, are endogenous GR ligands secreted by the adrenal gland which contribute to metabolic homeostasis including adaptation to fasting under the control of the hypothalamic–pituitary–adrenal (HPA) axis [20,21]. However, the effect of GR on the hepatic Klf15-1a expression remains unknown.

These findings prompted us to test the hypothesis that GR induces the hepatic Klf15-1a upregulation during fasting and also regulates hepatic lipogenesis through the KLF15-SREBP-1 pathway.

Results

GR-KLF15 pathway controls SREBP-1 and its downstream lipogenic genes

It is well-known that dexamethasone (Dex), as a GR ligand, elicits the expression of KLF15 in skeletal muscle and adipocytes [16–18]. Previously, we demonstrated that the liver-specific KLF15 variant, Klf15-1a, is highly expressed in the liver [14]. However, it has yet to be thoroughly examined whether GR and its ligand modulate the upregulation of Klf15-1a expression. Therefore, we conducted a study to investigate the hepatic Klf15-1a expression at 3 h following Dex administration.

As depicted in Fig. 1A, the expression of Klf15-1a was significantly upregulated following Dex administration. This finding is consistent with our previous report demonstrating that KLF15 suppresses SREBP-1 gene expression through the formation of a complex with RIP140-LXR on the SREBP-1 promoter [8], as indicated by the significant decrease in SREBP-1 expression seen in Fig. 1B. The results were consistent with those at the protein level (Fig. S1A). Concurrently, *Tat* (encoding tyrosine aminotransferase: TAT), a well-known target gene of GR, was significantly elevated (Fig. 1C), while the expression of GR (*Nr3c1*) remained unchanged (Fig. 1D), suggesting that these regulatory effects were a result of authentic ligand action. These observations were also confirmed in experiments using another GR ligand, hydrocortisone (HC) (Fig. S1B–D). The expression of *Hpd* (encoding 4-hydroxyphenylpyruvate dioxygenase: HPD), a prominent target gene of KLF15 involved in amino acid metabolism, was significantly increased at 6 h post-administration of Dex (Fig. 1E).

Subsequently, we examined the expression of SREBP-1 target genes involved in lipogenesis. *Acly* (encoding ATP-citrate lyase: ACL), *Acss2* (encoding cytoplasmic acetyl-coenzyme A synthetase: AceCS1), *Acaca*, and *Fasn*, all known to be target genes of SREBP-1 and encoding enzymes crucial for fatty acid synthesis, were investigated (Fig. 1F). As expected, given the suppression of SREBP-1 by Dex, these lipogenic genes were subsequently downregulated in the Dex-treated group (Fig. 1G–J). It is well-established that the downregulation of SREBP-1 and its downstream genes reduces hepatic triglyceride (TG) levels. Therefore, we evaluated the effect of Dex administration on hepatic TG levels. To prevent the influx of fat from the diet, mice were fed a fat-free diet for 4 days prior to Dex treatment. As a result, hepatic TG levels were significantly decreased (Fig. 1K).

KLF15 is the key to control of hepatic lipogenesis by GR

To further clarify the role of KLF15 in the suppression of SREBP-1 under Dex administration, we conducted experiments using *Klf15*^{−/−} (KLF15KO) mice (Fig. 2A). As shown in Fig. 2B–F, compared to *Klf15*^{+/+} (wild-type) mice, Dex administration did not significantly suppress the expression of *Srebf1* and *Hpd* genes in KLF15KO mice. In contrast, the response of *Tat* gene expression, a direct target of GR, was similar to that seen in wild-type mice. Furthermore, in line with the alteration of *Srebf1* expression, there were no reductions in the expression of downstream lipogenic genes or hepatic TG levels observed
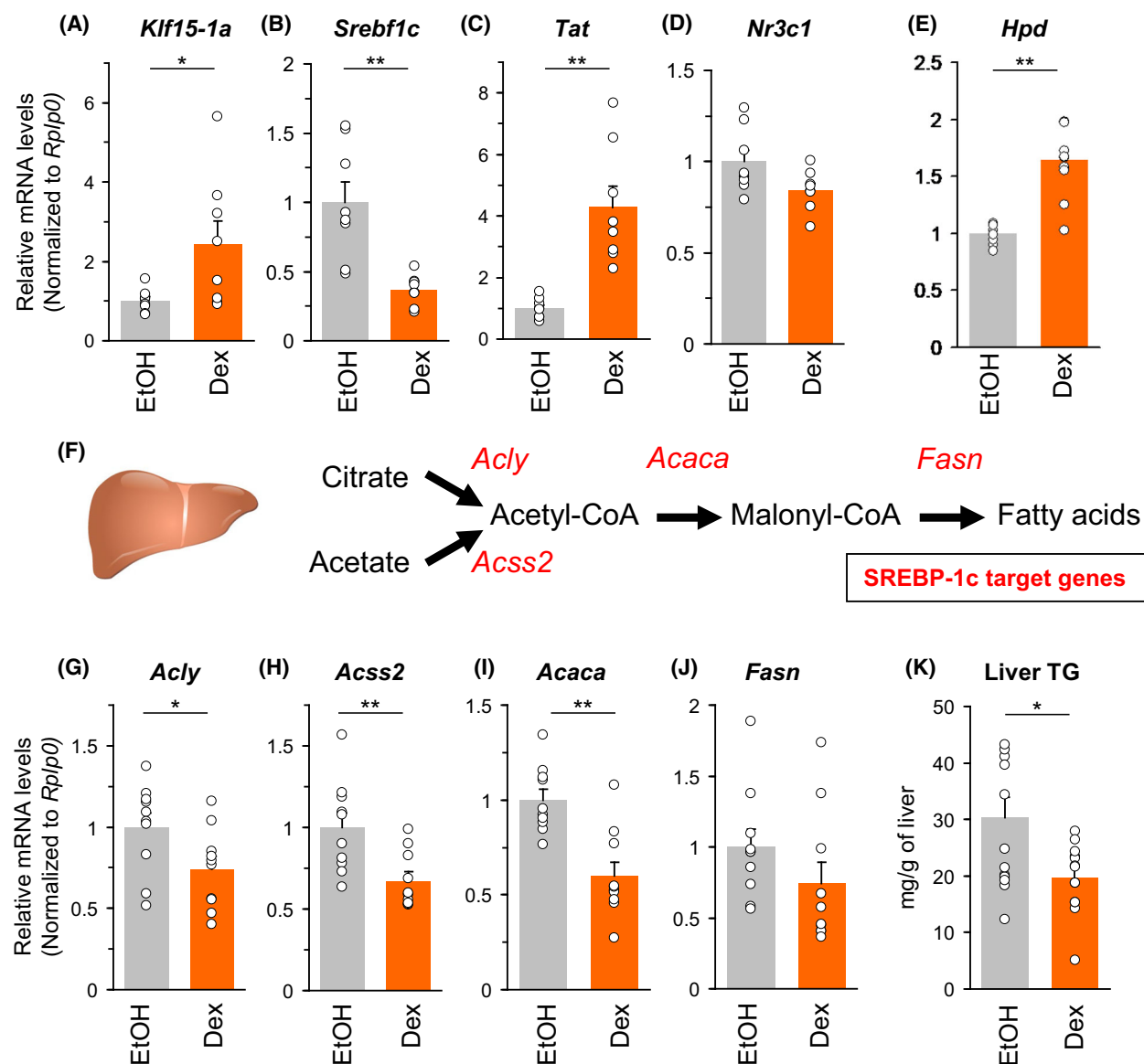
Fig. 1. GR-KLF15 pathway controls SREBP-1c and its downstream lipogenic genes. ICR male mice were intraperitoneally injected with dexamethasone at 1 mg·kg^{-1} body weight or vehicle. Both groups of mice were sacrificed at the same period in the light cycle to eliminate the effects of circadian rhythm on endogenous corticosterone levels. (A–D) Q-RT PCR analysis of liver RNA samples in Dex 3 h-treated mice ($n = 8$). *Tat* is known as direct target of GR. (E–J) Q-RT PCR analysis of liver RNA samples in Dex 6 h-treated mice ($n = 10$). (F) Schema of lipogenic pathway in liver. These genes, shown in red, are known to be regulated by SREBP-1. (K) Liver triglyceride levels of Dex 24 h-treated mice ($n = 13$). To avoid dietary fat effects, mice were fed a high-sucrose, fat-free diet for 4 days prior to Dex treatment. Data were assessed using the unpaired two-tailed Student's t-test. The differences were considered to be significant if $P < 0.05$ (*$P < 0.05$ and **$P < 0.01$). Error bars mean ± SEM.

in KLF15KO mice (Fig. 2G–K). These results demonstrate that KLF15 plays a key role in the regulation of hepatic lipogenesis by GR.

GR is involved in fasting response

In the liver, KLF15 is known to be upregulated during fasting. Therefore, we examined whether Cort, an endogenous mouse GR ligand, concurrently increases during fasting. As anticipated, plasma Cort levels were significantly higher after 24 h-fasting than after re–feeding (Fig. 3A). This change in Cort was accompanied by corresponding fluctuations in the expression levels of *Klf15*, *Srebf1*, and *Tat* (Fig. 3B–D). Additionally, we evaluated the binding ability of GR to the Klf15-1a enhancer under these nutritional conditions.
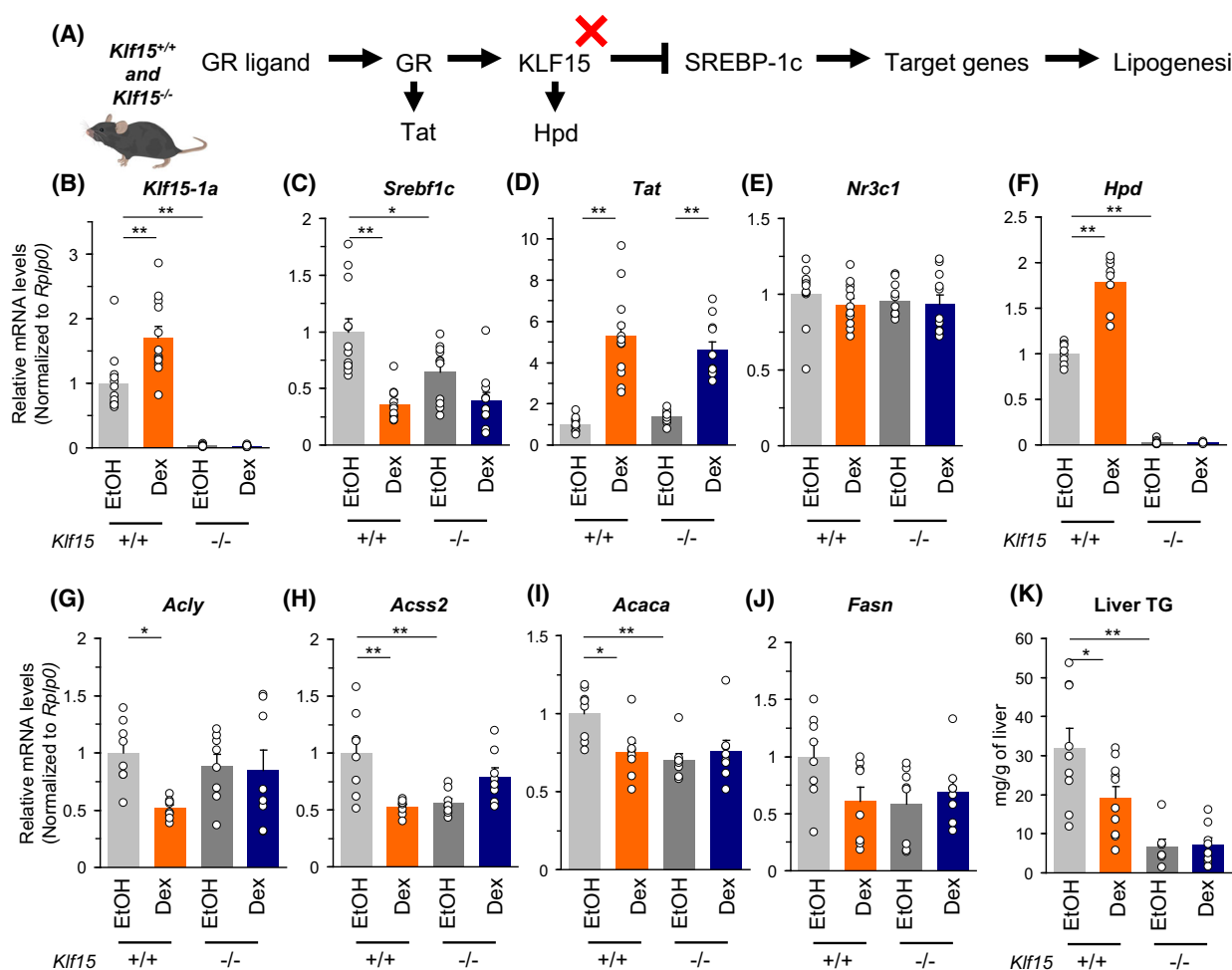
Fig. 2. KLF15 is the key to control of hepatic lipogenesis by GR. *Klf15*^{+/+} and *Klf*15[−/−] male mice were intraperitoneally injected with dexamethasone at 1 mg·kg^{−1} body weight or vehicle. Both groups of mice were sacrificed at the same period in the light cycle to eliminate the effects of circadian rhythm on endogenous corticosterone levels. (A) Schema of KLF15-SREBP-1-lipogenesis pathway in liver. (B–E) Q-RT PCR analysis of liver RNA samples in Dex 3 h-treated *Klf15*^{+/+} and *Klf15*^{−/−} mice (*n* = 11–12). (E–J) Q-RT PCR analysis of liver RNA samples in Dex 6 h-treated *Klf15*^{+/+} and *Klf15*^{−/−} mice (*n* = 8). (K) Liver triglyceride levels of Dex 24 h-treated *Klf15*^{+/+} and *Klf15*^{−/−} mice (*n* = 7–10). To avoid dietary fat effects, mice were fed a high-sucrose, fat-free diet for 4 days prior to Dex treatment. Datasets were assessed by ANOVA. The differences were considered to be significant if $P < 0.05$ (*$P < 0.05$ and **$P < 0.01$). Error bars mean ± SEM.

As shown in Fig. 3E,F, GR binding was significantly higher during fasting. These results were also corroborated by ChIP-seq analysis for GR in livers of fasted and re-fed mice obtained from the GEO database (GSE119713) (Fig. S2). It is worth noting that the levels of nuclear GR protein in the liver did not differ between fasting and re-feeding (Fig. 3G).

GR-binding element to control expression of liver-specific Klf15 transcript during fasting

We have previously identified the enhancer regions in *Klf15* gene that are necessary and sufficient for the fasting responses of Klf15-1a transcript [14]. The two

GR-binding elements (GREs) reported previously [16–18] were located within these regions. The DNA sequences of these two GREs (GRE1 and GRE2) are highly conserved among mammals (Fig. S3A–C). In addition, ChIP-seq results obtained from the GEO database (GSE119713) showed that the binding of GR to these GREs-containing region, especially near GRE1, was enhanced by Dex treatment (Fig. S3D). Previously, we generated an adenovirus vector containing a construct linking these important regions to a luciferase reporter gene (Ad-Klf15-1a-Luc-WT, previously referred to as C2 in Ref. [14]), and were successful in measuring the activation of the Klf15-1a in the liver during fasting. To clarify the importance of these
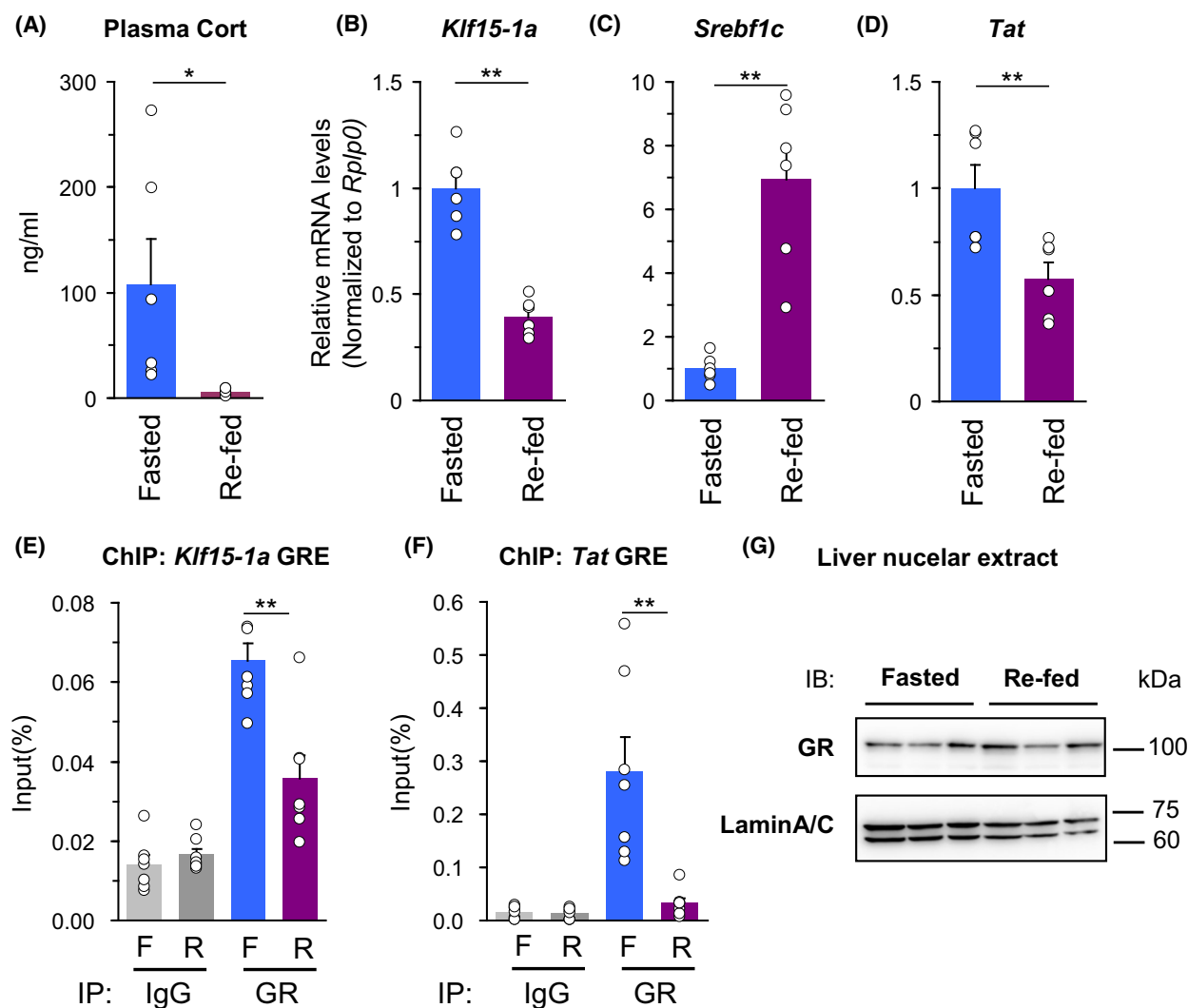
Fig. 3. GR is involved in fasting response. ICR male mice were fasted for 24 h or re-fed for 16 h after a 24 h fast. Both groups of mice were sacrificed at the same period in the early light cycle to eliminate the effects of circadian rhythm on endogenous corticosterone levels. (A) Plasma corticosterone levels in fasted and re-fed mice ($n = 6$). (B–D) Q-RT PCR analysis of liver RNA samples in fasted and re-fed mice ($n = 8$). (E, F) Elucidations of GR protein binding to Klf15 promoter in liver. ChIP assay was performed with anti-GR antibody and normal IgG as a control using liver samples of fasted and re-fed mice ($n = 7$). Klf15-1a GRE ChIP primer set detects both GRE1 and GRE2. This is because GRE1 and GRE2 are located close to each other on the genome. (G) Immunoblot analysis of GR using liver nuclear extracts from fasted and re-fed mice ($n = 3$). Lamin A/C was detected as an internal control for nuclear protein. Differences between two groups were assessed using the unpaired two-tailed Student's *t*-test. Datasets involving more than two groups were assessed by ANOVA. The differences were considered to be significant if $P < 0.05$ (*$P < 0.05$ and **$P < 0.01$). Error bars mean ± SEM.

GREs in fasting responses, we engineered Ad-Klf15-1a-Luc-WT with mutations in these GREs (Ad-Klf15-1a-Luc-GREmut, including mutations in both GREs) and measured hepatic enhancer activity using the *in vivo* Ad-luc method as previously described (Fig. 4A) [14]. As shown in Fig. 4B,C, the reporter activity of Ad-Klf15-1a-Luc-WT significantly increased in the fasted state and decreased in the re-fed state, while the response of the GREmut construct was significantly attenuated, suggesting that the GREs

regulate transcriptional activity through the effects of GR and its ligands during fasting. It was confirmed that this GREmut construct did not respond to GR ligands, Dex *in vivo* (Fig. 4D,E), and Cort in hepatoma cells (Fig. S4).

HPA axis is the driver of fasting response

To further verify the importance of an endogenous GR ligand for Klf15-1a gene expression, we performed
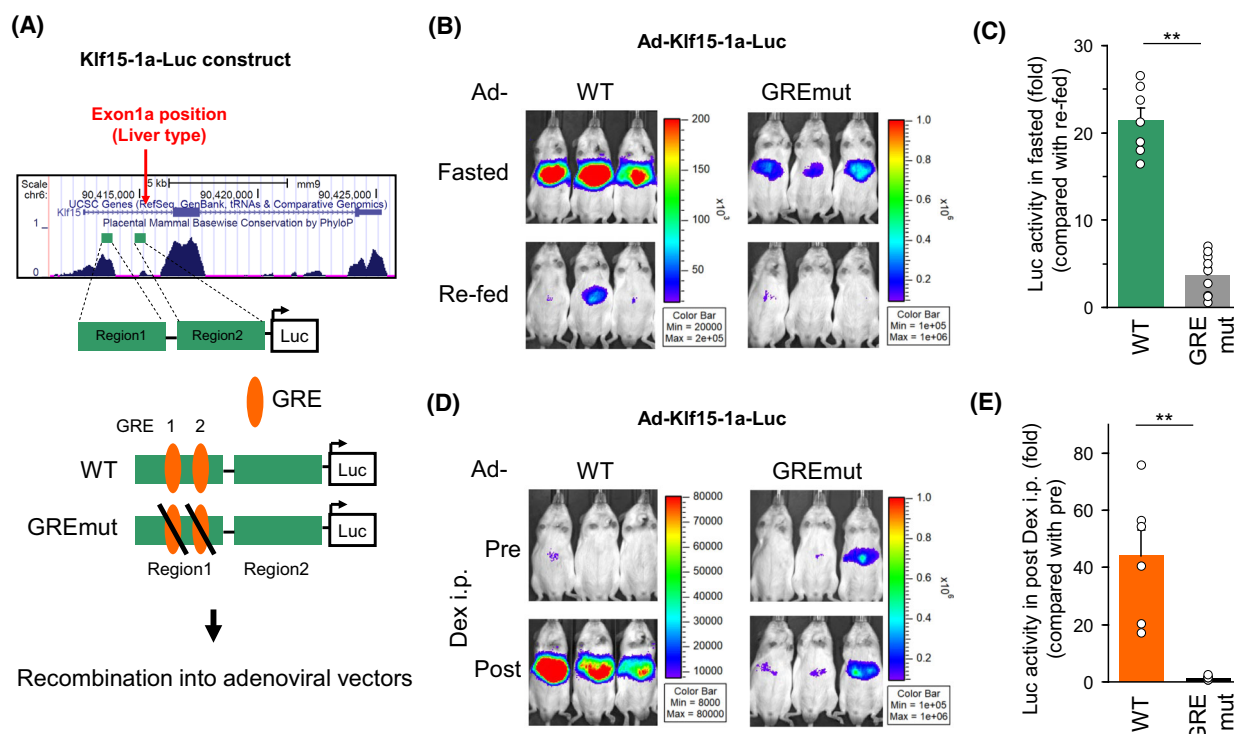
Fig. 4. GRE to control expression of liver-specific Klf15 transcript during fasting. (A) Structure of Klf15-1a-Luc construct. The enhancer regions of Klf15-1a transcript, which are important for fasting response are linked to the Luc reporter [14]. Two GR binding elements (GRE) are reported on the regions [16,18]. (B–E) *In vivo* Ad-luc promoter analyses using GR-binding element-mutated (GREmut) Ad-Klf15-Luc. Images (B, D) and hepatic luciferase activities (C, E) of mice injected with Ad-Klf15-Luc are shown (n = 6–9). The fasting (B, C) and post (6 h-treated)-Dex i.p. (D, E) promoter activities in the liver are expressed relative to activity in the re-fed state and pre-Dex i.p., respectively, to adjust for mouse-to-mouse differences in promoter expression in Ad-treated mice. Data were assessed using the unpaired two-tailed Student's t-test. The differences were considered to be significant if $P < 0.05$ (**$P < 0.01$). Error bars mean ± SEM.

experiments using adrenalectomy model mice (ADX). Because ADX mice were significantly weakened by long-term (24 h) fasting, we conducted the experiments using short-term (6 h) fasting. Our pilot study confirmed that plasma Cort and hepatic Klf15-1a expression were significantly higher during this fasting period of 6 h than ad lib states (Fig. S5A,B). As a result, plasma Cort concentrations in ADX mice were significantly lower than in sham operation mice (Sham) and Klf15-1a expression significantly decreased, similar to *Tat* (Fig. 5A–C).

Finally, we sought to determine if the downregulation of Klf15-1a mRNA levels in ADX mice was due to reduced enhancer activity using the *in vivo* Ad-luc reporter system with Ad-Klf15-1a-Luc-WT. As shown in Fig. 5D–G, short-term fasting significantly upregulated Klf15-1a enhancer activity in Sham mice, while the response in ADX mice was significantly lower in both absolute activity (Fig. 5F) and fold changes (Fig. 5G). ChIP-seq data using ADX mice obtained from the GEO database (GSE46047) confirmed that

depletion of plasma Cort attenuated GR binding on these GRE regions (Fig. S5C). These results suggest that the HPA axis is the driver of fasting responses (Fig. 6).

Discussion

This study demonstrates that the liver-specific variant of KLF15 is controlled through GR and its ligand during fasting, and subsequently, the metabolic flow between the macronutrients, especially regarding the conversion pathway from glucose to fatty acids, is regulated by this pathway (Fig. 6).

Dex, a synthetic GR ligand, significantly elevated Klf15-1a transcript in the liver (Fig. 1A) and concurrently decreased *Srebf1* gene expression (Fig. 1B). These results are consistent with our previous finding that KLF15 suppresses SREBP-1 expression in the liver [8]. To exclude the possibility of side effects of ethanol (EtOH), which was used as the solvent for Dex in Fig. 1, we administered HC, a water-soluble
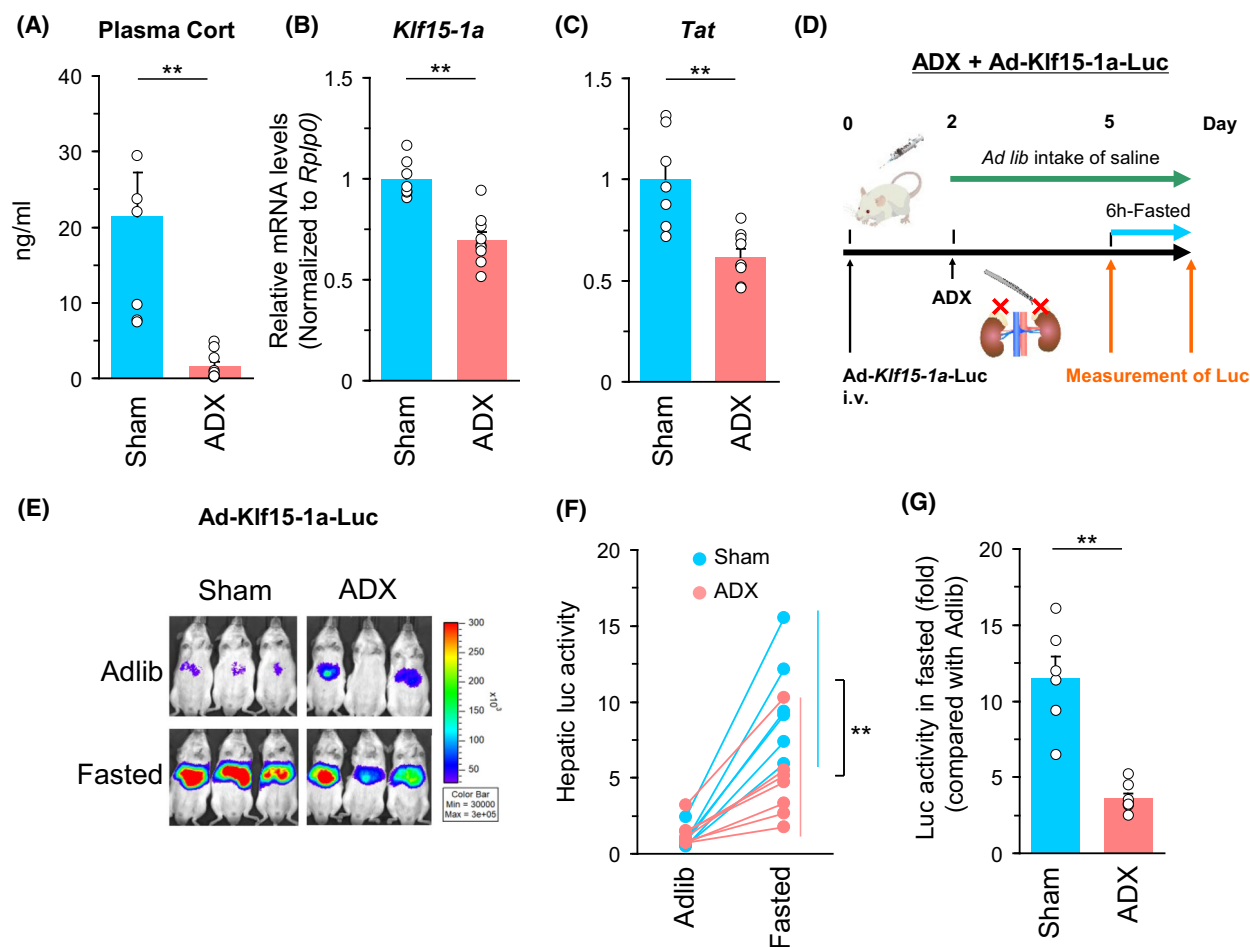
Fig. 5. HPA axis is the driver of fasting response. Three days after adrenalectomy (ADX) to reduce endogenous GR ligand (corticosterone in plasma), ADX mice and Sham mice were fasted for 6 h. Both groups of mice were sacrificed at the same period in the light cycle to eliminate the effects of circadian rhythm on endogenous corticosterone levels (A–C). (A) Plasma corticosterone levels in ADX mice ($n = 7$–9). (B, C) Q-RT PCR analysis of liver RNA samples in ADX mice ($n = 7$–9). (D) The experimental procedure for ADX mice for E–G. (E–G) *In vivo* Ad-luc promoter analyses using Ad-Klf15-Luc. Images (E), hepatic luciferase activities (F), and fold changes between Adlib and 6 h-fasted states (G) of mice injected with Ad-Klf15-Luc are shown ($n = 5$–6). The 6 h-fasted promoter activity in the liver is expressed relative to activity in the ad lib state, to adjust for mouse-to-mouse differences in promoter expression in Ad-treated mice (G). Data were assessed using the unpaired two-tailed Student's *t*-test. The differences were considered to be significant if $P < 0.05$ (**$P < 0.01$). Error bars mean ± SEM.

GR ligand, and obtained similar results (Fig. S1). The target genes of SREBP-1, such as *Acly*, *Acss2*, *Acaca*, and *Fasn* related to the fatty acid synthesis pathway, as well as hepatic TG levels in the liver, were significantly decreased phenotypically (Fig. 1G–K). Furthermore, Dex administration did not shut down the hepatic lipogenic pathway consisting of the SREBP-1 and its downstream targets in KLF15KO mice, supporting the dependence of this suppression effect on KLF15 (Fig. 2).

The ability of GR to bind to the Klf15-1a enhancer increased during fasting and decreased in the re-fed state (Fig. 3E), and the GR binding actually promoted transcription of the Klf15-1a (Fig. 4). Two mechanisms are known to regulate GR transcriptional activity by GR ligands: one is nuclear translocation of GR and the other is enhanced binding of GR to genomic DNA [22,23]. In the current fasting and re-feeding model, nuclear GR protein levels remained unchanged (Fig. 3G) between the transition, despite an increase in GR binding to target genes during fasting (Fig. 3E,F), indicating that elevated plasma corticosterone enhanced the binding of GR to genomic DNA.

In line with our finding, it has been reported that glucocorticoids modulate the expression of genes involved in lipid metabolism through gene expression
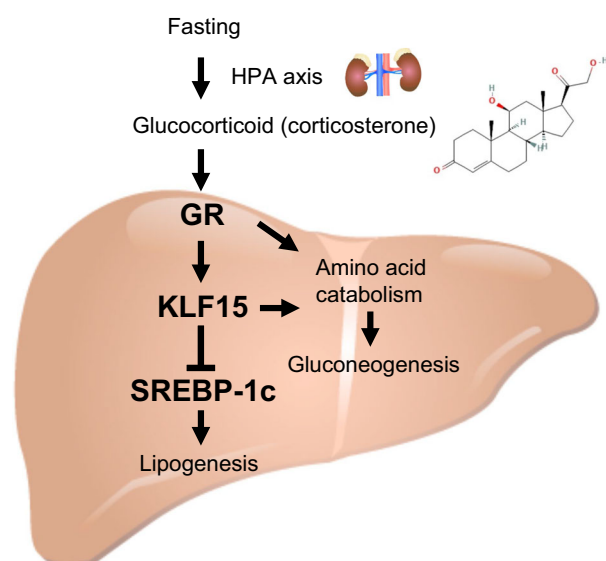
Fig. 6. GR-KLF15 pathway controls hepatic lipogenesis. Schematic representation of the molecular mechanism by which the GR-KLF15 axis controls hepatic lipogenesis and gluconeogenesis during fasting.

profiling in the livers of prednisolone-treated mice [24]. Additionally, it has been documented that GR suppresses lipogenesis through a decrease in the nuclear accumulation of SREBP-1 protein in the liver [25], although the proposed molecular mechanisms differ from those of the KLF15-dependent pathway. Consistently, it has been reported that a single administration of Dex decreased intrahepatic TG content, whereas multiple consecutive Dex treatments increased it [26]. Regarding the increase in TG content caused by multiple consecutive Dex treatments, it is suggested that it is primarily attributable to increased lipolysis in adipose tissue due to glucocorticoid stimulation, resulting in increased circulating fatty acids that are converted to triglycerides in the liver [27].

Previously, we identified the mechanism by which KLF15 suppresses SREBP-1 transcription as its interaction with the LXR/RXR/RIP140 complex [8]. Administration of Dex did not suppress SREBP-1 expression in KLF15KO mice, demonstrating that the suppressive effect of glucocorticoids on SREBP-1 and thereby hepatic lipogenesis is mediated by KLF15 (Fig. 2). It is notable that KLF15KO mice exhibited lower liver TG levels at baseline compared to the WT mice (Fig. 2K). It may be related to lower blood glucose, which serves as a substrate for hepatic TG synthesis, and higher plasma glucagon, which is known to reduce hepatic TG [28], in KLF15KO mice compared to WT mice [10,29]. Whatever the reason, this fact

does not imply a minor contribution of KLF15 in the regulation of the fasting response [8].

Glucocorticoid receptor has been known to play a crucial role in the regulation of KLF15 expression in skeletal muscle, where the GR-KLF15 pathway transactivates E3 ubiquitin ligase genes, atrogin-1 and MuRF1, and negatively modulates myofiber size [16]. It also upregulates key enzymes involved in the breakdown of branched-chain amino acids, thereby providing gluconeogenic substrates to the liver [10]. Given that KLF15 activates gluconeogenesis in the liver, the GR-KLF15 pathway serves to metabolically link skeletal muscle to the liver during fasting.

The secretion of glucocorticoids is regulated by the HPA axis. The HPA axis plays numerous important roles in the body, including the regulation of metabolism, immune function, and stress response [30,31]. In response to stress, the hypothalamus releases corticotropin-releasing hormone, which stimulates the pituitary gland to secrete adrenocorticotropic hormone (ACTH). ACTH then activates the adrenal glands to release glucocorticoids, which play a significant role in the metabolic response to undernutrition by causing an increased release of amino acids from skeletal muscle and their subsequent conversion to glucose in the liver [32–34]. Increased levels of plasma ACTH and glucocorticoids during fasting have been found in humans [35,36] and rodents [34,37,38]. Given that GREs in the KLF15 gene are critical for the fasting response and are highly conserved across various mammalian species (Fig. S3), it is suggested that the GR-KLF15 pathway plays a role of great significance beyond evolution.

Overall, these findings demonstrate that the HPA-axis-regulated GR-KLF15 pathway plays a crucial role in the regulation of lipid metabolism in the liver during fasting.

Materials and methods

Materials

Anti-GR (sc-393232), anti-KLF15 (sc-271675), anti-lamin A/C (sc-376248) mouse monoclonal antibodies, and control mouse IgG (sc-2025) were purchased from Santa Cruz Biotechnology Inc. (Santa Cruz, CA, USA) Anti-SREBP-1 rabbit polyclonal antibody was described previously [4]. Dexamethasone (Dex) and corticosterone (Cort) were purchased from Wako Pure Chemical Industries (Osaka, Japan) and were dissolved in ethanol as a 5 mg·mL^{-1} stock solution. Hydrocortisone sodium succinate (HC) was purchased from Sigma-Aldrich (St. Louis, MO, USA) and was dissolved in water as a 5 mg·mL^{-1} stock solution. Cort ELISA kit (Item No. 501320) was purchased from Cayman Chemical (Ann Arbor, MI, USA).

Animals

Five to seven-week-old ICR male mice were purchased from Japan SLC, Inc. (Shizuoka, Japan) $Klf15^{-/-}$ (KLF15KO) mouse on C57BL/6 background was kindly gifted by M. K. Jain and genotyped as previously described [39]. The experiments using ICR were performed between 6 and 8 weeks of age, and the experiments using $Klf15^{+/+}$ (wild-type) and $Klf15^{-/-}$ mice were performed at 5–6 months of age, respectively. All mice were maintained in a temperature-controlled environment with a 14 h-light/10 h-dark cycle. All mice had free access to a standard diet (MF; Oriental Yeast, Tokyo, Japan) and water. For the fasting group, animals were starved 24 h, and for the re-feeding group, they were re-fed for 16 h after a 24 h starvation. For the experiments with Dex- and HC-treated mice, the mice were given an intraperitoneal (i.p.) injection of the reagents at 1 mg·kg^{-1} body weight and sacrificed after the indicated periods as previously described [40]. Adrenalectomy (ADX) was performed in ICR male mice using the dorsal approach under a three-type mixed anesthesia consisting of domitol, midazolam, and betorfal as previously described [40]. Both adrenal glands were removed from the mice with anti-bleeding measures and the surgical incisions were sutured using 5–0 Silk Suture (K890H; Ethicon, Somerville, NJ, USA). Sham operation mice (Sham) were the same as ADX except that the adrenal glands were not removed. After the surgery, the mice were given free access to a standard diet, water, and saline. For the experiments of liver TG measurement, mice were fed a high-sucrose fat-free diet (Oriental Yeast) for 4 days prior to Dex administration. Liver TG levels were measured using TG E-test Wako kit (FUJIFILM Wako Pure Chemical, Osaka, Japan) as described previously [5]. Mice were sacrificed in the light phase in the indicated states. All animals studied were anesthetized and euthanized according to the protocol approved by the Tsukuba University Animal Care and Use Committee (#22-066). All experiments were repeated at least twice to correct the bias for each experimental environment.

RNA isolation and quantitative reverse transcription PCR

Total RNA preparation from mouse liver was performed with Sepasol-RNA I Super G (Nacalai Tesque, Kyoto, Japan) as previously described [14]. Briefly, 500 ng of total RNA was reverse transcribed in a volume of 5 μL and converted to cDNA using the ReverTra Ace qPCR RT Master Mix (TOYOBO, Osaka, Japan). Quantitative reverse transcription PCR (Q-RT PCR) was performed using KAPA SYBR Fast qPCR Kit (NIPPON Genetics, Tokyo, Japan) on a QuantStudio™ 5 Real-Time PCR System (Thermo Fisher Scientific, Waltham, MA, USA) and quantified using the standard curve method with cDNA as template.

After amplification by PCR, samples containing the product with the correct Tm value were taken based on the melting curve plot for each sample. The primer sets are listed in Table S1. *Rplp0* was used as the correction of the gene expression level for each sample.

In vivo imaging of luciferase activity

In vivo imaging was performed as described previously [14,41,42]. Four days after the adenovirus transduction, mice were fasted for 24 h after early dark phase and then re-fed for 16 h. In the Dex experiments, mice were treated with Dex for 6 h in the ad lib state within the light phase. For the ADX mice experiments, 2 days after adenovirus transduction, ADX was performed, and on the 3rd day, mice were fasted for 6 h within the light phase. At each condition, D-luciferin dissolved in PBS at a concentration of 7.5 mg·mL^{-1} was intraperitoneally injected at a dose of 10 mL·kg^{-1} into mice and the luminescence in the liver was captured using an IVIS™ Imaging System (PerkinElmer, Waltham, MA, USA). Relative photon emission over the liver region was quantified using LIVING IMAGE™ software (PerkinElmer). Hepatic transduction efficiency was determined based on the quantification of adenoviral DNA in the liver using a previously described Q-PCR method [43], and the result of quantification was used to normalize the *in vivo* imaging of luciferase activity. Two paired data from the same animal on the different conditions was continuously obtained and the ratio between the two quantities was used to cancel the variations in hepatic transduction efficiencies. Results of hepatic luminescence less than 5×10^4 counts·min^{-1} (1.22×10^6 photons) on both conditions were not adopted due to inadequate detection accuracy.

Chromatin immunoprecipitation assay

Chromatin immunoprecipitation (ChIP) assays using mouse liver were performed as described previously [14]. Briefly, 100 mg of liver tissue samples from the fasted and re-fed mice were minced in 1 mL of PBS and cross-linked in 1.5% formaldehyde for 15 min at room temperature. Fixed samples were homogenized and then subjected to sonication with Bioruptor2 (Sonicbio, Kanagawa, Japan) for DNA fragmentation. After centrifugation, supernatant was diluted to 6 mL with dilution buffer (50 mM Tris–HCl at pH 8.0, 167 mM NaCl, 1 mM EDTA, 1.1% Triton X-100, and 0.11% sodium deoxycholate) and then 1 mL of total volume was used for immunoprecipitation with 1 μg of anti-GR antibody or with 1 μg of control IgG bound to 30 μL of Dynabeads magnetic beads (Thermo Fisher Scientific) and rotated overnight at 4 °C. Fifty microliter of total volume was used for input sample. The complexes were washed with low-salt wash buffer (50 mM Tris–HCl at pH 8.0, 150 mM NaCl, 1 mM EDTA, 1% Triton X-100,

0.1% SDS, and 0.1% sodium deoxycholate), high-salt wash buffer (50 mM Tris–HCl at pH 8.0, 500 mM NaCl, 1 mM EDTA, 1% Triton X-100, 0.1% SDS, and 0.1% sodium deoxycholate), LiCl wash buffer (10 mM Tris–HCl at pH 8.0, 0.25 M LiCl, 1 mM EDTA, 0.5% NP40, and 0.5% sodium deoxycholate), and TE buffer. DNA–protein complex was eluted by incubation with elution buffer (1% SDS, 0.1 M NaHCO₃) for 15 min at room temperature, and then incubated with 200 mM NaCl overnight at 65 °C for reverse crosslinking. DNA–protein complex was treated with 200 μg·mL^{-1} proteinase K, and chromatin DNA was purified with phenol–chloroform, eluted in TE buffer, and subjected to Q-PCR analysis. From reverse crosslinking step, the input sample was also subjected to the same procedure. Q-PCR was performed using the same method as Q-RT PCR and quantified by standard curve method with input DNA samples. The primer sets are listed in Table S2.

Immunoblotting

Immunoblotting was performed as described previously [14]. Nuclear extract protein from mouse liver was prepared as previously described [44–46].

Preparation and transduction of recombinant adenoviruses

Recombinant adenoviruses Ad-Klf15-1a-Luc-WT were prepared as described previously [14]. The mutated Klf15-1a-Luc-GREm plasmids were generated using PrimeSTAR Mutagenesis Basal Kit (Takara Bio Inc., Tokyo, Japan) based on PCR according to the mutation method [16,18]. The primer sets were 5′-*CAACATGTTCA*TCCTACAGCCGCTGTGTC-3′ and 5′-*TGAACATGTT*GTTGATAACAAGCCGAGAG-3′ for GRE1, and 5′-*AAGCTT*GGG*AAGCTT*CTCCCCCTGCACGCAGCC-3′ and 5′–*AAGCTT*CCC*AAGCTT*GGGCACGGTCCCCGGCAG-3′ for GRE2. Italics indicate GRE mutation sites. Adenoviral construct Ad-Klf15-1a-Luc-GREm was generated by homologous recombination between the entry vector based on Klf15-1a-Luc-GREm and the pAd promoterless vector (Thermo Fisher Scientific). Recombinant adenoviruses were propagated in HEK293 cells and purified by CsCl gradient centrifugation as described previously [43]. For animal experiments, adenoviruses were injected intravenously into ICR male mice from subclavian vein at the following doses: for Klf15-1a-Luc-WT, 4×10^7 P.F.U.; for Klf15-1a-GREm-Luc, 2×10^8 P.F.U., and 1000 optical particles of adenovirus were calculated as 1 P.F.U.

Cell culture

HEK293 human embryonic kidney cells (RRID: CVCL_0045) and HepG2 human hepatoma cells (RRID: CVCL_0027) were distributed from ATCC (American Type Culture Collection, Manassas, VA, USA), and cultured in DMEM containing 25 mM glucose, 100 U·mL^{-1} penicillin, and 100 μg·mL^{-1} streptomycin sulfate supplemented with 10% FBS. All cell lines have been authenticated by our facility's authentication protocol within the last 3 years, and all experiments were performed with mycoplasma-free cells.

Luciferase assay

For luciferase assay, HepG2 cells were seeded in a 48-well plate and incubated to 10–20% confluent. The indicated amounts of expression plasmids, firefly luciferase reporter plasmid, and Renilla luciferase reporter plasmid (pRL-SV40; Promega, Madison, WI, USA) were co-transfected into cells using Lipofectamin3000 reagent (Thermo Fisher Scientific) according to the manufacturer's protocol. The Myc-GR expression plasmid was generated as described previously [40]. Total amounts of transfected DNA were adjusted with empty plasmid. After transfection, Cort was added to the medium and the cells were cultured. After 24 h, the cells were lysed. The luciferase activity in transfectants was measured as described previously [8]. Renilla luciferase activities were used to normalize transfection efficiencies. The luciferase activity in transfectants was then measured using a luminometer with a firefly luciferase assay reagent (Toyo Bnet bio, Tokyo, Japan) and a Renilla luciferase assay reagent (Promega).

Statistical analyses

Data are expressed as means ± SEM. Differences between two groups were assessed using the unpaired two-tailed Student's *t*-test. Data sets involving more than two groups were assessed using ANOVA, when indicated by appropriate *P*-values ($P < 0.05$), by Tukey–Kramer *post hoc* test, with STATVIEW Software (BrainPower, Calabasas, CA, USA). The differences were considered to be significant if $P < 0.05$ (*$P < 0.05$ and **$P < 0.01$).

Conflict of interest

The authors declare no conflict of interest.

Author contributions

YT conceived the experiments, performed the experiments, analyzed the data, and co-wrote the paper. YM, YA, ZMS, SK, DT, KK, CY, AS, YM, YI, TMi, TMa, YK, and HS discussed the results and interpretation of data and commented on the manuscript. NY conceived the experiments, analyzed the data, and co-wrote the paper.

Peer review

The peer review history for this article is available at https://www.webofscience.com/api/gateway/wos/peer-review/10.1111/febs.16957.

Data availability statement

Data supporting the findings of this study are available from the corresponding author upon reasonable request.

References

1 Hall KD, ed. (2012) Quantitative Physiology of Human Starvation: Adaptations of Energy Expenditure, Macronutrient Metabolism and Body Composition. Springer, Berlin.

2 Yokoyama C, Wang X, Briggs MR, Admon A, Wu J, Hua X, Goldstein JL & Brown MS (1993) SREBP-1, a basic-helix-loop-helix-leucine zipper protein that controls transcription of the low density lipoprotein receptor gene. *Cell* **75**, 187–197.

3 Shimano H, Horton JD, Shimomura I, Hammer RE, Brown MS & Goldstein JL (1997) Isoform 1c of sterol regulatory element binding protein is less active than isoform 1a in livers of transgenic mice and in cultured cells. *J Clin Invest* **99**, 846–854.

4 Shimano H, Yahagi N, Amemiya-Kudo M, Hasty AH, Osuga J, Tamura Y, Shionoiri F, Iizuka Y, Ohashi K, Harada K *et al.* (1999) Sterol regulatory element-binding protein-1 as a key transcription factor for nutritional induction of lipogenic enzyme genes. *J Biol Chem* **274**, 35832–35839.

5 Yahagi N, Shimano H, Hasty AH, Amemiya-Kudo M, Okazaki H, Tamura Y, Iizuka Y, Shionoiri F, Ohashi K, Osuga J *et al.* (1999) A crucial role of sterol regulatory element-binding protein-1 in the regulation of lipogenic gene expression by polyunsaturated fatty acids. *J Biol Chem* **274**, 35840–35844.

6 Yahagi N, Shimano H, Hasty AH, Matsuzaka T, Ide T, Yoshikawa T, Amemiya-Kudo M, Tomita S, Okazaki H, Tamura Y *et al.* (2002) Absence of sterol regulatory element-binding protein-1 (SREBP-1) ameliorates fatty livers but not obesity or insulin resistance in Lep(ob)/Lep(ob) mice. *J Biol Chem* **277**, 19353–19357.

7 Horton JD, Bashmakov Y, Shimomura I & Shimano H (1998) Regulation of sterol regulatory element binding proteins in livers of fasted and refed mice. *Proc Natl Acad Sci USA* **95**, 5987–5992.

8 Takeuchi Y, Yahagi N, Aita Y, Murayama Y, Sawada Y, Piao X, Toya N, Oya Y, Shikama A, Takarada A *et al.* (2016) KLF15 enables rapid switching between lipogenesis and gluconeogenesis during fasting. *Cell Rep* **16**, 2373–2386.

9 Teshigawara K, Ogawa W, Mori T, Matsuki Y, Watanabe E, Hiramatsu R, Inoue H, Miyake K, Sakaue H & Kasuga M (2005) Role of Kruppel-like factor 15 in PEPCK gene expression in the liver. *Biochem Biophys Res Commun* **327**, 920–926.

10 Gray S, Wang B, Orihuela Y, Hong EG, Fisch S, Haldar S, Cline GW, Kim JK, Peroni OD, Kahn BB *et al.* (2007) Regulation of gluconeogenesis by Kruppel-like factor 15. *Cell Metab* **5**, 305–312.

11 Takashima M, Ogawa W, Hayashi K, Inoue H, Kinoshita S, Okamoto Y, Sakaue H, Wataoka Y, Emi A, Senga Y *et al.* (2010) Role of KLF15 in regulation

of hepatic gluconeogenesis and metformin action. *Diabetes* **59**, 1608–1615.

12 Jeyaraj D, Scheer FA, Ripperger JA, Haldar SM, Lu Y, Prosdocimo DA, Eapen SJ, Eapen BL, Cui Y, Mahabeleshwar GH et al. (2012) Klf15 orchestrates circadian nitrogen homeostasis. *Cell Metab* **15**, 311–323.

13 Fan L, Hsieh PN, Sweet DR & Jain MK (2018) Kruppel-like factor 15: regulator of BCAA metabolism and circadian protein rhythmicity. *Pharmacol Res* **130**, 123–126.

14 Takeuchi Y, Yahagi N, Aita Y, Mehrazad-Saber Z, Ho MH, Huyan Y, Murayama Y, Shikama A, Masuda Y, Izumida Y et al. (2021) FoxO-KLF15 pathway switches the flow of macronutrients under the control of insulin. *iScience* **24**, 103446.

15 Yahagi N & Takeuchi Y (2021) Genome-wide screening of upstream transcription factors using an expression library. *F1000Res* **10**, 51.

16 Shimizu N, Yoshikawa N, Ito N, Maruyama T, Suzuki Y, Takeda S, Nakae J, Tagata Y, Nishitani S, Takehana K et al. (2011) Crosstalk between glucocorticoid receptor and nutritional sensor mTOR in skeletal muscle. *Cell Metab* **13**, 170–182.

17 Morrison-Nozik A, Anand P, Zhu H, Duan Q, Sabeh M, Prosdocimo DA, Lemieux ME, Nordsborg N, Russell AP, MacRae CA et al. (2015) Glucocorticoids enhance muscle endurance and ameliorate Duchenne muscular dystrophy through a defined metabolic program. *Proc Natl Acad Sci USA* **112**, E6780–E6789.

18 Asada M, Rauch A, Shimizu H, Maruyama H, Miyaki S, Shibamori M, Kawasome H, Ishiyama H, Tuckermann J & Asahara H (2011) DNA binding-dependent glucocorticoid receptor activity promotes adipogenesis via Kruppel-like factor 15 gene expression. *Lab Invest* **91**, 203–215.

19 Kennedy CLM, Price EM, Mifsud KR, Salatino S, Sharma E, Engledow S, Broxholme J, Goss HM & Reul J (2023) Genomic regulation of Kruppel-like-factor family members by corticosteroid receptors in the rat brain. *Neurobiol Stress* **23**, 100532.

20 Muglia L, Jacobson L, Dikkes P & Majzoub JA (1995) Corticotropin-releasing hormone deficiency reveals major fetal but not adult glucocorticoid need. *Nature* **373**, 427–432.

21 Opherk C, Tronche F, Kellendonk C, Kohlmuller D, Schulze A, Schmid W & Schutz G (2004) Inactivation of the glucocorticoid receptor in hepatocytes leads to fasting hypoglycemia and ameliorates hyperglycemia in streptozotocin-induced diabetes mellitus. *Mol Endocrinol* **18**, 1346–1353.

22 Dahlman-Wright K, Wright A, Carlstedt-Duke J & Gustafsson JA (1992) DNA-binding by the glucocorticoid receptor: a structural and functional analysis. *J Steroid Biochem Mol Biol* **41**, 249–272.

23 Schauer M, Chalepakis G, Willmann T & Beato M (1989) Binding of hormone accelerates the kinetics of glucocorticoid and progesterone receptor binding to DNA. *Proc Natl Acad Sci USA* **86**, 1123–1127.

24 Frijters R, Fleuren W, Toonen EJ, Tuckermann JP, Reichardt HM, van der Maaden H, van Elsas A, van Lierop MJ, Dokter W, de Vlieg J et al. (2010) Prednisolone-induced differential gene expression in mouse liver carrying wild type or a dimerization-defective glucocorticoid receptor. *BMC Genomics* **11**, 359.

25 Roqueta-Rivera M, Esquejo RM, Phelan PE, Sandor K, Daniel B, Foufelle F, Ding J, Li X, Khorasanizadeh S & Osborne TF (2016) SETDB2 links glucocorticoid to lipid metabolism through Insig2a regulation. *Cell Metab* **24**, 474–484.

26 Letteron P, Fromenty B, Terris B, Degott C & Pessayre D (1996) Acute and chronic hepatic steatosis lead to in vivo lipid peroxidation in mice. *J Hepatol* **24**, 200–208.

27 Mir N, Chin SA, Riddell MC & Beaudry JL (2021) Genomic and non-genomic actions of glucocorticoids on adipose tissue lipid metabolism. *Int J Mol Sci* **22**, 8503.

28 Perry RJ, Zhang D, Guerra MT, Brill AL, Goedeke L, Nasiri AR, Rabin-Court A, Wang Y, Peng L, Dufour S et al. (2020) Glucagon stimulates gluconeogenesis by INSP3R1-mediated hepatic lipolysis. *Nature* **579**, 279–283.

29 Jung DY, Chalasani U, Pan N, Friedline RH, Prosdocimo DA, Nam M, Azuma Y, Maganti R, Yu K, Velagapudi A et al. (2013) KLF15 is a molecular link between endoplasmic reticulum stress and insulin resistance. *PLoS One* **8**, e77851.

30 Smith SM & Vale WW (2006) The role of the hypothalamic-pituitary-adrenal axis in neuroendocrine responses to stress. *Dialogues Clin Neurosci* **8**, 383–395.

31 Herman JP, McKlveen JM, Ghosal S, Kopp B, Wulsin A, Makinson R, Scheimann J & Myers B (2016) Regulation of the hypothalamic-pituitary-adrenocortical stress response. *Compr Physiol* **6**, 603–621.

32 Munck A, Guyre PM & Holbrook NJ (1984) Physiological functions of glucocorticoids in stress and their relation to pharmacological actions. *Endocr Rev* **5**, 25–44.

33 Tischler ME, Henriksen EJ & Cook PH (1988) Role of glucocorticoids in increased muscle glutamine production in starvation. *Muscle Nerve* **11**, 752–756.

34 Woodward CJ, Hervey GR, Oakey RE & Whitaker EM (1991) The effects of fasting on plasma corticosterone kinetics in rats. *Br J Nutr* **66**, 117–127.

35 Beer SF, Bircham PM, Bloom SR, Clark PM, Hales CN, Hughes CM, Jones CT, Marsh DR, Raggatt PR & Findlay AL (1989) The effect of a 72 h fast on plasma levels of pituitary, adrenal, thyroid, pancreatic and gastrointestinal hormones in healthy men and women. *J Endocrinol* **120**, 337–350.

36 Nakamura Y, Walker BR & Ikuta T (2015) Systematic review and meta-analysis reveals acutely elevated plasma cortisol following fasting but not less severe calorie restriction. *Stress* **19**, 151–157.

37 Makimura H, Mizuno TM, Isoda F, Beasley J, Silverstein JH & Mobbs CV (2003) Role of glucocorticoids in mediating effects of fasting and diabetes on hypothalamic gene expression. *BMC Physiol* **3**, 5.

38 Maeda N, Fujiki J, Hasegawa Y, Ieko T, Miyasho T, Iwasaki T & Yokota H (2022) Testicular induced corticosterone synthesis in male rats under fasting stress. *Steroids* **177**, 108947.

39 Fisch S, Gray S, Heymans S, Haldar SM, Wang B, Pfister O, Cui L, Kumar A, Lin Z, Sen-Banerjee S *et al.* (2007) Kruppel-like factor 15 is a regulator of cardiomyocyte hypertrophy. *Proc Natl Acad Sci USA* **104**, 7074–7079.

40 Murayama Y, Yahagi N, Takeuchi Y, Aita Y, Mehrazad Saber Z, Wada N, Li E, Piao X, Sawada Y, Shikama A *et al.* (2019) Glucocorticoid receptor suppresses gene expression of Rev-erbα (Nr1d1) through interaction with the CLOCK complex. *FEBS Lett* **593**, 423–432.

41 Takeuchi Y, Yahagi N, Izumida Y, Nishi M, Kubota M, Teraoka Y, Yamamoto T, Matsuzaka T, Nakagawa Y, Sekiya M *et al.* (2010) Polyunsaturated fatty acids selectively suppress sterol regulatory element-binding protein-1 through proteolytic processing and autoloop regulatory circuit. *J Biol Chem* **285**, 11681–11691.

42 Mehrazad Saber Z, Takeuchi Y, Sawada Y, Aita Y, Ho MH, Karkoutly S, Tao D, Katabami K, Ye C, Murayama Y *et al.* (2021) High protein diet-induced metabolic changes are transcriptionally regulated via KLF15-dependent and independent pathways. *Biochem Biophys Res Commun* **582**, 35–42.

43 Takeuchi Y, Yahagi N, Nakagawa Y, Matsuzaka T, Shimizu R, Sekiya M, Iizuka Y, Ohashi K, Gotoda T, Yamamoto M *et al.* (2007) In vivo promoter analysis on refeeding response of hepatic sterol regulatory element-binding protein-1c expression. *Biochem Biophys Res Commun* **363**, 329–335.

44 Sheng Z, Otani H, Brown MS & Goldstein JL (1995) Independent regulation of sterol regulatory element-binding proteins 1 and 2 in hamster liver. *Proc Natl Acad Sci USA* **92**, 935–938.

45 Yahagi N, Shimano H, Matsuzaka T, Najima Y, Sekiya M, Nakagawa Y, Ide T, Tomita S, Okazaki H, Tamura Y *et al.* (2003) p53 activation in adipocytes of obese mice. *J Biol Chem* **278**, 25395–25400.

46 Yahagi N, Shimano H, Matsuzaka T, Sekiya M, Najima Y, Okazaki S, Okazaki H, Tamura Y, Iizuka Y, Inoue N *et al.* (2004) p53 involvement in the pathogenesis of fatty liver disease. *J Biol Chem* **279**, 20571–20575.

Supporting information

Additional supporting information may be found online in the Supporting Information section at the end of the article.

Fig. S1. Effects of GR ligands on KLF15 in the liver.
Fig. S2. ChIP-seq with anti-GR antibody.
Fig. S3. Information on GREs on the Klf15 promoter.
Fig. S4. Effect of Cort on KLF15 promoter activity in HepG2 cells.
Fig. S5. Effect of GR ligand on Klf15 expression during short-term fasting.
Table S1. List of primer sets used for Q-RT PCR.
Table S2. List of primer sets used for ChIP assay.